Published in final edited form as:
Arterioscler Thromb Vasc Biol. 2010 July ; 30(7): 1378–1388. doi:10.1161/ATVBAHA.109.200428.

Targeted *Vezf1* null mutation impairs vascular structure formation during ES cell differentiation

Zhongmin Zou[1,#], **Pauline A. Ocaya**[2,#], **Huiquin Sun**[1], **Frank Kuhnert**[1], and **Heidi Stuhlmann**[1,2,*]

[1]Department of Cell Biology, Division of Vascular Biology, The Scripps Research Institute, La Jolla, CA

[2]Department of Cell and Developmental Biology, Weill Cornell Medical College, New York, NY

Abstract

Objective—*Vezf1* is an early zinc finger transcription factor that is essential for normal vascular development and functions in a dose-dependent manner. Here, we investigated the role of *Vezf1* during processes of endothelial cell differentiation and maturation by studying mutant *Vezf1* ES cells using the in vitro embryoid body differentiation model and the in vivo teratocarcinoma model.

Methods and Results—*Vezf1*−/− ES cell-derived embryoid bodies failed to form a well-organized vascular network and showed dramatic vascular sprouting defects. Our results indicate that the retinol pathway is an important mediator of *Vezf1* function, and that loss of *Vezf1* results in reduced retinol/Vitamin A signaling and aberrant extracellular matrix formation. Unexpectedly, we also uncovered defects during in vitro differentiation of *Vezf1*−/− ES cells along hematopoietic cell lineages. *Vezf1*−/− ES cell-derived teratocarcinomas were able to spontaneously differentiate into cell types of all three germ layers. However, histological and immunohistochemical examination of these tumors showed decreased cell proliferation, delayed differentiation, and large foci of cells with extensive deposition of extracellular matrix. Embryoid bodies and teratocarcinomas derived from heterozygous ES cells displayed an intermediate phenotype.

Conclusion—Together, these results suggest that *Vezf1* is involved in early differentiation processes of the vasculature by regulating cell differentiation, proliferation, and ECM distribution and deposition.

Keywords

Vezf1; zinc finger gene; vascular development; gene knock-out; ES cells; embryoid body differentiation; teratocarcinoma

*Corresponding author: Department of Cell and Developmental Biology Weill Cornell Medical College 1300 York Avenue New York, NY 10021 Tel. 212-746-6156 Fax 212-746-8175 hes2011@med.cornell.edu .
#The first two authors contributed equally to the manuscript
Present addresses: Department of Toxicology, State Key Laboratory of Burn, Trauma and Combined Injury, Third Military Medical University, Chongqing, P.R.China 400038 (Z.Zou, H.Sun)
Department of Medicine, Division of Hematology, Stanford University Medical Center, Stanford, CA 94305, USA (F.Kuhnert)

Disclosure. The authors declare that they have no relationships that could be perceived as real or apparent conflicts of interest.

Introduction

Development of the vascular system involves two distinct processes: coalescence of mesoderm-derived angioblasts to form a primitive vascular plexus (vasculogenesis); and subsequently sprouting, branching, remodeling, and maturation of the primary plexus to give rise to the mature blood vasculature (angiogenesis) [1-3]. These complex developmental processes require the precise temporal and spatial expression of a large number of genes. Much progress has been made over the past 15 years to identify relevant genes, and to understand their participation in signaling pathways and their role in vascular development and disease [1, 4, 5]. In contrast, much less is understood about how the precise expression of vascular-specific genes is mediated by the coordinated action of transcription factors. Promoter analysis of endothelial-specific genes in vitro identified crucial transcriptional regulatory factors. Their roles in vascular development and in the adult endothelium have been elucidated through transgenic and gene targeting studies (reviewed in [6-8]). The emerging picture from these studies suggests that most if not all transcription factors that are important for blood vessel formation are not endothelial-specific either in their expression or in their function. In fact, several of these factors are involved in both hematopoiesis and vascular development. Furthermore, expression of endothelial genes during blood vessel formation and homeostasis often requires unique combinations of multiple transcription factors, possibly in combination with tissue-specific co-factors or bridging proteins [6, 7].

In a gene trap screen for early cardiovascular genes, we have identified a novel zinc finger transcription factor, *Vezf1* [9-11]. The C2H2 (Krüppel-like) zinc finger protein VEZF1 is highly conserved among vertebrates, and its 518 amino acid sequence shows only six amino acid differences between mouse and human [12], suggesting that *Vezf1* plays a conserved role in mammals. *Vezf1* is unique amongst endothelial transcription factors: although it is expressed in the endothelium as well as in neuronal and mesodermal tissues [10, 13], its function appears to be restricted to the vascular system. In vitro studies indicate that *Vezf1* regulates the proliferation, migration and network formation of endothelial cells [14]. In addition, its human ortholog DB1/ZNF161 functionally interacts with Rho GTPases and associated regulatory proteins and regulates expression of the human endothelin-1 gene [15-17]. Targeted inactivation of *Vezf1* in mice results in embryonic lethality at midgestation, and *Vezf1* was found to control development of the blood vascular and lymphatic system in a dose-dependent fashion [18]. Homozygous mutant embryos showed defects in vascular remodeling and loss of vascular integrity resulting in localized hemorrhaging, concomitant with defects in endothelial cell adhesion and junction formation in the mutant vessels. Haploinsufficiency was observed in 20% of heterozygous embryos, and those displayed lymphatic hypervascularization associated with hemorrhaging and edema.

Here, we address the specific role(s) of *Vezf1* in endothelial cell proliferation, sprouting, and remodeling by using an in vitro differentiation assay of mutant ES cells into embryoid bodies (EB). Vasculogenesis and angiogenesis occur in successive steps during EB formation, and these can be easily followed by using immunohistochemical methods [19-22], making this in vitro model suitable for studies of targeted mutations in ES cells [20, 23, 24]. In addition, pluripotent ES cells, when transplanted into an ectopic location in syngeneic or athymic host mice, can develop tumors of different tissue types called teratocarcinoma [25]. We have employed this in vivo differentiation model to examine *Vezf1* gene function during tissue differentiation and tumor development. Our results show that *Vezf1* is involved in multiple processes of vascular formation by regulating cell differentiation, proliferation, as well as ECM distribution and deposition.

Methods

ES cell culture, EB differentiation, and angiogenic sprouting assay

Wild-type R1 ES cells (wt; *Vezf1*+/+), *Vezf1*+/− (clone V2) and *Vezf1*−/− ES cells (clone F3) [18] were maintained on γ-irradiated primary mouse embryo fibroblast (MEF) feeder cells in high-glucose DMEM (Gibco BRL) supplemented with 20% fetal bovine serum (FBS; Gemini), 0.1 mM β-mercaptoethanol, 1 mM L-glutamine, 0.1 mM non-essential amino acids, 20mM HEPES and 1,000 U/ml of LIF (ESGRO; Chemicon, USA). In vitro differentiation of ES cells into embryoid bodies (EBs) was initiated using the hanging drop culture protocol [20]. Briefly, drops containing ES cells (2,500 cells in 30 μl) were spotted onto the lid of 150-mm dishes and incubated as "hanging drops" in DMEM supplemented with 10% FBS (Atlas Biologicals), β-mercaptoethanol, L-glutamine, non-essential amino acids and HEPES as described above, in the absence of LIF. EBs were collected after 2 days and grown in suspension culture between 1 to 12 days before harvesting. Alternatively, EBs grown for 2 days in hanging drops were cultured for 1 day in suspension and then transferred to 2D attachment cultures on gelatin-coated tissue culture plates for spontaneous differentiation. Lymphatic endothelial cell (LEC) differentiation was induced in EBs at day-5 or day-14 in suspension culture by adding 20ng/ml recombinant human VEGF-A165 (R&D Systems) and 200ng/ml recombinant human VEGF-C (R&D Systems) [26, 27], and cultured for up to 21 days post induction. At indicated time points, EBs were collected, fixed in 4% paraformaldehyde, and embedded in OCT. Angiogenic sprouting assays were performed in semi-solid 3-D collagen gels [21]. Briefly, EBs from day-12 suspension culture were harvested, embedded in type I collagen gel containing 20 ng/ml VEGF and cultured in small droplets for 2 to 5 days. EBs were fixed in situ, transferred to glass slides, air-dried, and stored at −20°C for immunostaining.

Immunofluorescence and immunohistochemistry

Protocols for immunofluorescence and immunohistochemistry were essentially as described [18]. Primary antibodies used were rat anti-mouse PECAM-1/CD31 (1:200; Pharmingen), rat anti-mouse MECA-32 (1:15; Pharmingen), ICAM-1 (1:100; Seikagaku Corp.), goat anti-mouse VE-cadherin (1:20; R&D Systems), rabbit anti-mouse collagen IV (1:200; Chemicon), rabbit anti-human Caspase-3 (1:200; Cell Signaling Technology, Inc.), rabbit Annexin V (1:200; Abcam), and rabbit anti-mouse LYVE1 (1:200; AngioBio). For each antibody, an IgG isotype antibody was used as a control. Secondary antibodies included TRITC-conjugated goat anti-rabbit IgG, $F(ab')_2$, FITC-conjugated goat anti-rat IgG (1:100), Cy3-conjugated donkey anti-rat IgG (1:300), Cy3-conjugated goat anti-rabbit IgG (1:300), Cy5-conjugated donkey anti-goat IgG (1:500), HRP-conjugated donkey anti-rabbit IgG (1:200), and HRP-conjugated donkey anti-rabbit IgG(H+L) (1:200). Nuclei were counterstained with DAPI using Vectashield mounting medium (Vector Labs). Images were taken under a Zeiss Axioplan 2 IE MOT microscope using digital ORCA-ER-1394 camera.

Quantitative RT-PCR

Total RNA was extracted from ES cells following MEF depletion and from day-5 EBs using TRIzol Reagent (Invitrogen). cDNA was prepared from 1 μg RNA using Superscript III Reverse Transcriptase and random hexamers (Invitrogen) in a 40 μl reaction. A 1:20 aliquot of the cDNA reaction was used for Real Time PCR in a 25-μl reaction using SYBR Green technology (Applied Biosystems). Gene expression was measured on a BioRad IQ5 Multicolor PCR Cycler (BioRad) using primers listed below, and was normalized using primers against mouse β-actin. To confirm specificity of the reaction, melting point analysis was incorporated at the end of the PCR.

Gene	Forward Primer	Reverse primer	Product size in bp
RBP4	gacaaggctcgtttctctgg	aaaggaggctacaccccagt	243
TTR	gacaggatggcttcccttcg	ccaggactttgaccatcagagg	117
RAR-β	gcctgcagaagtgctttgaagt	gctttccggatcttctcagtga	150
Aldh2	gagcaggggcctcaggtgga	tcattggcccgccccacaac	248
Col-IV(a)1	ttcagattccgcagtgcccta	ttctcatgcacacttggcagc	310
Col-IV(a)2	tggctgaggaggaaatcaagc	aatggcgttgcacggaagt	232
β-actin	gtgggccgctctaggcaccaa	ctctttgatgtcacgcacgatttc	539

Protein isolation and western blots

Conditioned medium was collected, filtered, and snap frozen from wt and *Vezf1*−/− ES cells cultured for 24 hours, and from EBs maintained in medium supplemented with 50ng/mL VEGF-A and 100ng/mL bFGF (R&D Systems). Protein concentration was determined by using the BCA™ Protein Assay (Pierce, IL). 50μg of protein from conditioned media was separated on 4-12% SDS-polyacrylamide gels and transferred to nitrocellulose membranes (Whatman GmbH, Dassel) using the NUPAGE® Electrophoresis and Transfer System (Invitrogen, CA). Pre-stained low range molecular weight standard (Invitrogen, CA) and purified RBP4 (kind gift from Dr. William Blaner, Columbia University) were also included. Membranes were blocked in 2% skim milk in Tris-buffered saline (0.05% Tween 20; 1 hour at room temperature) and incubated overnight with rabbit polyclonal anti-RBP4 antibody (1:500; provided by Dr. William Blaner, Columbia University). Secondary antibody used was horseradish peroxidase-conjugated donkey anti rabbit (1:5000, 1 hour at room temperature). The ECL Plus Western Blotting Reagent (Amersham Biosciences) was used to visualize RBP4 protein.

Flow Cytometry

At indicated time points, EBs and undifferentiated ES cells were dissociated to single-cell suspension using 0.2% collagenase A (Sigma). Dissociated ES cells were MEF-depleted by incubation on gelatin-coated dishes (0.7%; Sigma). ES cells and EB-derived cells were fixed in 2% paraformaldehyde and washed in staining buffer (0.01% NaN_3 in PBS). For oct3/4 expression, cells were incubated with 1% saponin (Sigma) for 15 minutes prior to washing. Cells were incubated for Fc receptor blockage with rat anti-mouse CD16/CD32 (1μg/10^6 cells) and stained either alone with Alexa647-conjugated rat anti-mouse Oct3/4 (1μg/10^6 cells; eBiosciences) or in combination with PE-CY7-conjugated rat anti-mouse PECAM-1/CD31 (0.5μg/10^6 cells; e-Biosciences), Alexa 488-conjugated rat anti-mouse VE-Cadherin (1μg/10^6 cells; eBiosciences) and PE-conjugated rat anti-mouse CD41 (1μg/10^6 cells; Becton-Dickinson Biosciences). Cells were washed, re-suspended in PBS then filtrated using cell-strainer caps. Unstained cells were used to set the cut-off for background fluorescence. Data acquisition was done using FACs Canto (Becton-Dickinson Bioscience) and analysis was performed using FlowJo Software.

Generation of ES cell clones with LacZ knock-in into the Vezf1 locus

The original Vezf1 targeting construct contained a deletion of the transcription start site, resulting in a non-functional LacZ gene [18]. A new construct termed $Vezf1^{lacZ}$ was generated, in which the transcriptional start site was restored and the IRES-lacZgt1.2neo cassette was replaced by an SDK-lacZ-PGKneo cassette. XhoI-linearized DNA was introduced into R1 ES cells by electroporation, and six correctly targeted clones were identified by Southern blot

analysis as described [18]. Expression of LacZ in EB derived from targeted ES cell clones was detected by using a b-galactosidase staining kit (Activemotif, CA).

Teratocarcinoma formation

A total of 1×10^7 cells of clone F3 (*Vezf1*−/−) or clone V2 (*Vezf1*+/−) suspended in 150μl PBS was injected subcutaneously into the left flank of 6- to 8-week old male nude mice. The right flank was injected with wt ES cells as a control. Two weeks after injection, animals were sacrificed, and the teratocarcinomas were dissected from the subcutaneous fascial planes, weighed and fixed overnight in 4% paraformaldehyde. Half of each teratocarcinoma was embedded in OCT and the other half in paraffin, sectioned at 6 μm and used for immunostaining or H&E staining, respectively. The weight of each individual control teratocarcinoma was used as 100%, and the weight of the experimental teratocarcinoma from the same animal was expressed as percentage of the control. A total of six mice were used for each ES cell clone.

Results

Delayed attachment and reduced growth of *Vezf1*−/− EBs

To investigate in detail the role of *Vezf1* during vascular development, we examined the formation of vascular structures in EBs derived from ES cells that are homozygous (*Vezf1*−/−), heterozygous (*Vezf1*+/−), or wild type (wt) for a targeted *Vezf1* null allele [18]. We have shown previously that *Vezf1* mRNA is absent in *Vezf1*−/− ES cells and EBs, and reduced to about half in *Vezf1*+/− EBs [18]. The in vitro differentiation of ES cells was initiated in hanging drop cultures, followed by growth either in suspension culture or in 2D attachment culture. We first assessed the ability of EB to attach to substrate and for outgrowth of differentiating cells. After overnight culture on gelatin-coated dishes, almost all EBs derived from *Vezf1*+/− and wt ES cells were attached and had formed a rim of spreading, differentiating cells, whereas about one-third of *Vezf1*−/− EBs did not firmly attach overnight, or even within 6 days of culture (not shown). Furthermore, cellular outgrowth from those *Vezf1*−/− EBs that attached to the culture dishes was significantly delayed and slower, with diameters of attached *Vezf1*−/− EBs about 50% reduced compared to *Vezf1*+/− and wt EBs (Fig. 1A). Interestingly, when grown in suspension culture, mutant and wt EBs formed cystic structures; however, both *Vezf1*+/− and *Vezf1*−/− EBs grew significantly slower than wt EBs, and by day-6 they were about 1/3 smaller compared to wt controls (Fig. 1B).

Vascular structure defects in mutant *Vezf1* EBs

We next examined the differentiation of endothelial cells and formation of vascular structures in EBs. For this, EBs were grown in 2D attachment culture and double-stained at day-3, -6, -9, and -12 with antibodies specific for the mouse pan-endothelial marker PECAM-1/CD31 and the ECM protein collagen type IV. Differences between mutant and wt EBs became apparent at day-6 when endothelial cell cords were beginning to develop, and were most obvious at day 9 (shown in Fig. 2A). Thus, wt (*Vezf1*+/+) EBs displayed cords with PECAM-1/collagen IV positive endothelial cells that were organized into extensive vascular networks (Fig. 2A, left panel). In contrast, *Vezf1*−/− EBs formed only short PECAM-1 positive cell cords that did not develop into a proper vascular network. Overall, vascular coverage, as measured by the area covered by PECAM-1 positive structures, was reduced from 14.5% in wt to 3.6% in *Vezf1*−/− EBs (Fig. 2B). In addition, most of the PECAM-1 staining in *Vezf1* null EBs was localized in patches of cells with undifferentiated morphology (Fig. 2A, top right panel). High levels of collagen IV expression were visible on large sheets of undifferentiated cells (Fig. 2A, bottom right panel), and generally did not co-localize with PECAM-1 expression (35% co-localization of PECAM-1 and collagen IV in *Vezf1*−/− EBs vs. 98% in wt EBs; Fig. 2C). No changes in vascular structure formation were detected when 2D cultures were extended to 12 days, indicating that the observed defects were not due to delayed vascular differentiation.

Interestingly, *Vezf1*+/− EBs displayed an intermediate phenotype with shortened and thickened cell sheets that contained PECAM-1/collagen IV positive cells; however these had failed to form an extensive vascular network (Fig. 2A, middle panel).

We also examined vascular differentiation in EBs grown for 3, 6, and 9 days in suspension culture (representative sections of day-9 cystic EBs are shown in Fig. 2D). PECAM-1 and collagen IV in wt and *Vezf1*+/− EBs co-localized to endothelial cell cords that were mostly restricted to a region underneath an outer layer of tightly packed visceral endodermal cells (Fig. 2D, left and middle panel). These vascular structures were well developed. In contrast, *Vezf1*−/− EBs contained a broad, presumably mesodermal layer that was filled with collagen IV-positive cells but devoid of PECAM-1-positive cells. PECAM-1 positive cells were restricted to the center of the EBs, but these failed to coalesce into cords (Fig. 2D, right panel).

The expression patterns in wt and mutant EBs of endothelial ICAM-1 in 2D attachment culture (Suppl. Fig. 1), and of endothelial VE-cadherin (Suppl. Fig. 2) and MECA-32 (not shown) in suspension culture, respectively, was similar to that observed for PECAM-1. Thus, we observed patches of endothelial cells that lack to properly form vascular cords. VE-cadherin staining partially overlapped with PECAM-1 in *Vezf1* null EBs (Suppl. Fig. 2, bottom row). Together, these results confirm that endothelial lineage determination and differentiation is unaffected but that vascular structure formation is defective in EBs derived from *Vezf1*−/− ES cells. To test for the possibility that apoptosis could be the cause of the observed vascular defects, EBs were grown for 9 days in 2D attachment culture and co-stained for PECAM-1 and Caspase 3. However, no increase in the numbers of Caspase 3-positive cells was detected within the PECAM-1 positive cell population, or overall in the EBs (Suppl. Fig. 3). Similarly, when sections of day-9 suspension culture EBs were stained for Annexin V, we observed no increase in apoptosis in PECAM-1 positive or negative cells in mutant *Vezf1* EBs (Suppl. Fig. 4).

Finally, we investigated the formation of lymphatic endothelial structures in EBs derived from wt and mutant *Vezf1* ES cells. LYVE-1+/MECA-32− or LYVE-1+/PECAM-1+ cells became apparent in about 80% of wt EBs at day-7 in suspension culture and were found up to day-26 in cord-like structures. Fewer LYVE-1 positive EBs were obtained from *Vezf1*+/− and *Vezf1*−/− ES cells and at later time points of suspension culture. No obvious differences in the morphology of the putative lymphatic structures were found (data not shown).

Suppression of retinol metabolism in *Vezf1*−/− EBs

A recent microarray screen for *Vezf1* target genes in E9.5 embryos identified several candidate genes involved in retinol metabolism [28]. Specifically, expression of retinol binding protein 4 (Rbp4), a retinol/Vitamin A carrier in the plasma, and transthyretin (Ttr), which binds to RBP4 and prevents it from renal clearance [29, 30], was significantly decreased in *Vezf1*−/− embryos. Intriguingly, several studies reported that all-trans-retinoic acid inhibits collagen type IV expression in vitro in human and rat cells [31-33]. To investigate if expression of key retinol pathways genes and collagen IV are similarly affected during in vitro differentiation in mutant EBs, we performed quantitative RT-PCR on ES cells and day-5 EB. Expression of Rbp4, Ttr and the retinoic acid target gene RAR-β[34, 35] was significantly reduced in *Vezf1*−/− day-5 EBs but not in undifferentiated ES cells (Fig. 2E, left panel). The levels of secreted RBP4 protein were also decreased in supernatant medium harvested from *Vezf1*−/− EBs, and to a lesser extent in ES cells, when compared to wt controls (Fig. 2F). Consistent with the observed strong and aberrant immunostaining (Fig. 2A and D), increased expression of α1 and α2 chains of collagen type IV was detected in *Vezf1*−/− EBs (Fig. 2E, right panel). Together, these results support our model (Fig. 2G) that *Vezf1* activates the retinol/vitamin A pathway, either directly by transactivation of Rbp4 and Ttr, or indirectly. Deregulation of retinol/vitamin A signaling in *Vezf1* null EBs results in elevated collagen IV expression and accumulation (Fig. 2G).

Sprouting angiogenesis is impaired in *Vezf1−/−* EBs

When ES-derived EBs are embedded in a three-dimensional matrix of type I collagen in the presence of angiogenic factors, sprouting outgrowth of endothelial cells from the initial cord-like vascular structures in EBs can be observed that closely mimics sprouting angiogenesis in the developing embryo [36, 37]. The three-dimensional system is a powerful tool to study this angiogenesis process on a cellular and molecular level. To examine the ability of endothelial cells derived from *Vezf1* null ES cells to undergo sprouting angiogenesis, EBs were grown in suspension culture for 12 days and subsequently embedded in collagen type I gels in the presence of the pro-angiogenic growth factor VEGF. Generally, initial spouting was detected after 24 hours in wt and *Vezf1*+/− EBs in the collagen matrix. The sprouts continued to grow in number and length, and after 3-4 days the primary sprouts began to interconnect and formed secondary sprouts. Co-immunostaining for PECAM-1 and collagen IV of day-5 cultures indicated that the sprouts contained endothelial cells (Fig. 3A, left and middle column, and Fig. 3B). In contrast, no or few sprouts were visible after 24 hours in collagen-embedded *Vezf1* −/− EBs. At day-5 in collagen matrix, *Vezf1*−/− EBs had significantly fewer primary sprouts and rarely formed secondary sprouts (Fig. 3A, right column, and Fig. 3B). In conclusion, sprouting angiogenesis of mutant ES cell-derived endothelial cells was severely impaired.

Quantitative analysis of undifferentiated, endothelial, hematopoietic cell populations

We further examined the differentiation potential of wt and *Vezf1* mutant ES cells along the endothelial and hematopoietic lineages by using flow cytometry. Cell suspensions of wt, *Vezf1* +/− and *Vezf1*−/− ES cells and of day-9 EBs were analyzed for the presence of undifferentiated cells (Oct3/4-positive fraction), endothelial cell lineage (PECAM-1 positive and VE-cadherin positive fractions), and hematopoietic cell lineage (CD41 fraction) (Fig. 4). Wt and *Vezf1* mutant ES cells were able to differentiate at comparable levels, as judged by a similar decrease in Oct-3/4-positive cells (6- to 8-fold decrease during 9 days of in vitro differentiation; upper left panels in Fig. 4). Importantly, we did not detect a significant difference in endothelial marker gene expression between wt and mutant cells, as shown by the percentage of PECAM-1 positive and VE-cadherin positive cells before and after differentiation (Fig. 4, bottom panels). Thus, loss-of-function of *Vezf1* does not appear to block endothelial lineage determination and differentiation. We noted a 1.6-fold increase in VE-cadherin-positive cells with all three genotypes. We also observed an overall 3- to 4-fold decrease in PECAM-1 positive cells upon differentiation; the large fraction of PECAM-1 positive ES cells is consistent with its previously reported expression in the inner cell mass of blastocysts [38]. Unexpectedly, significantly lower numbers of CD41-positive hematopoietic cells were detected upon differentiation in *Vezf1* mutant EBs as compared to wt EBs. Thus, whereas the fraction of CD41-positive cells increased during wt EB differentiation by 19-fold, and during Vezf1+/− EB differentiation by 4-fold, no significant change was found during differentiation of *Vezf1*−/− EBs (0.75% vs. 0.85% $CD41^+$ cells; Fig. 4, upper right panel). To determine which specific hematopoietic lineages are affected, hematopoietic progenitor assays [39, 40] were performed (Suppl. Fig. 5). Day-6 EBs derived from wt and *Vezf1*+/− ES cells gave rise to all types of hematopoietic progenitors with similar efficiencies, including primitive erythroid, definitive erythroid, macrophage, bipotential definitive erythroid/macrophage, and multipotential precursor colonies. In contrast, greatly reduced numbers of primitive erythroid and bipotential colonies, and no definitive erythroid, macrophage, and multipotential progenitor colonies were obtained from *Vezf1*−/− day-6 EBs. Together, these results indicate that *Vezf1* null ES cells differentiate efficiently in vitro into PECAM-1 positive and VE-cadherin positive endothelial cells, but that differentiation into cells of the hematopoietic lineages is compromised.

Aberrant cell differentiation in teratocarcinomas derived from Vezf1-null ES cells

To study the differentiation of mutant *Vezf1* ES cells in vivo, *Vezf1*−/− or *Vezf1*+/− ES cells were transplanted subcutaneously into one flank of athymic nude mice, and wt ES cells were injected as control into the opposite flank. Two weeks later, teratocarcinomas were dissected, weighted and fixed. The growth of *Vezf1*−/− tumors and, to a lesser extend, of *Vezf1*+/− tumors was significantly reduced compared to wt controls (35% and 58% of wt control weight, respectively) (Fig. 5A). H&E staining of tumor sections revealed that both mutant and wt-derived teratocarcinomas contained a spectrum of somatic tissues derived from ecto-, endo- and mesoderm; these included epithelium, ciliatum, cartilage, bone, muscle cells, adipose tissue, neural and connective tissues (Fig. 5B). Overall, neural tissue was prominent in the tumors and consisted of neural rosettes and tubes, and central nervous system (CNS)-like tissue. In addition, an abundance of columnar epithelial cells lining cystic spaces formed glands and solid nests (Fig. 5B). Although *Vezf1*−/− ES cells were able to differentiate into every cell type found in the control teratocarcinomas, we detected notable differences. First, neural tube structures in *Vezf1*−/− teratocarcinomas were typically less differentiated (Fig. 5C), whereas wt tumors contained neural tissue of the more differentiated CNS-like phenotype. A second pathological feature was the large number of ECM-rich foci in connective tissue present in *Vezf1*−/− tumors, some of which formed bone-like structures (Fig. 5C). In contrast, wt tumors contained overall more gland-like structures with well-defined spaces that were surrounded by columnar epithelium, similar to those shown in the far right panel of Fig. 5B.

Reduced blood vessel formation in teratocarcinomas

We generated ES cell clones with a *LacZ* knock-in into the endogenous *Vezf1* locus (*Vezf1*$^{lacZ/+}$) (Suppl. Fig. 6). This approach allowed us to visualize *Vezf1* gene expression during in vivo and in vitro differentiation. β-galactosidase staining of *Vezf1*$^{lacZ/+}$ EBs grown in 2D attachment culture revealed that *Vezf1* expression was widespread but not ubiquitous. Prior to day-7, *LacZ* expression was highest located in the center of attached EBs in presumably mesodermal cells. Beginning at day-8 in culture, localized and elevated expression became apparent in cell clusters and tubes similar in appearance and shape to PECAM-1 positive structures, suggesting that these correspond to areas of early endothelial differentiation (Suppl. Fig. 6, bottom).

Teratocarcinomas derived from *Vezf1*−/− ES cells were smaller, and they contained fewer and less organized vascular structures that co-stained with PECAM-1 and Collagen IV when compared to wt or *Vezf1*+/− tumors (Fig. 6, and not shown). In addition, vascular structures in mutant teratocarcinomas rarely displayed ZO-1 positive cells (not shown). This prompted us to investigate if blood vessels in teratocarcinomas are derived from the host, from differentiating ES cells, or both. For this, we injected *Vezf1*$^{lacZ/+}$ ES cells into nude mice, allowing us to visualize ES cell-derived cells in the blood vessels. Sections from the resulting tumors were examined for co-localization of PECAM-1 and collagen IV immunostaining with β-galactosidase staining. The majority of PECAM-1 positive small vessels and the surrounding tissue were negative for *LacZ* (Fig. 5D, upper panel) and thus were presumably host-derived. However, a small portion of PECAM-1 positive cells within the vascular structures showed β-galactosidase activity, and these cells were interspersed with apparently host-derived endothelial cells within the same vessel (Fig. 5D, arrows in lower panel). Thus, our results suggest that *Vezf1* null ES cells are capable to differentiate into endothelial cells and to contribute to the formation of vessels within the teratocarcinomas.

Strikingly, distinct areas in *Vezf1*−/− ES cell-derived teratocarcinomas displayed low cellularity and high ECM content, as evidenced by H&E staining (Fig. 5C; Fig. 6, far right *Vezf1*−/−panel). In consecutive sections, these regions showed high levels of collagen IV deposition but few PECAM-1 positive cells, indicating rudiment and disorganized vascular

structures (Fig. 6). In contrast, wild-type teratocarcinomas contained well-organized vascular structures with PECAM-1 and collagen IV co-localization in ECM-rich regions (Fig. 6, *Vezf1* +/+ panels). These areas were similar in their morphology to mesenchymal or connective tissue where the majority of blood vessels are normally localized. The area density of blood vessels in wt and *Vezf1*−/− ES derived teratocarcinomas was 21.59±2.54% and 6.67±4.50%, respectively ($P<0.01$). Since the majority of the vessels are host-derived, indirect, non-endothelial effects may contribute to the reduced vascularity. The results suggest that the cellular microenvironment inside the teratocarcinomas may play an additional role in the formation of the tumor vasculature.

Discussion

Blood vessel development during mammalian embryogenesis is a finely tuned process that is controlled by a wide variety of genes. We have recently reported on the crucial and dosage-dependant role of the zinc finger transcription factor gene *Vezf1* during vascular system development [18]. Although *Vezf1* is expressed in the endothelium of the developing vasculature and in mesodermal and neuronal cells, the primary defect in *Vezf1* null embryos appears to have its origin in the endothelium. Thus, ultrastructural and immunohistochemical studies demonstrated loss of vascular wall integrity concomitant with defects in endothelial cell junctions and the ECM as the underlying cause of hemorrhaging and embryonic death [18]. In this study, we investigated in greater detail the involvement of *Vezf1* in various processes of angiogenesis. We used ES cells that are heterozygous or homozygous for a targeted *Vezf1* allele, and induced their differentiation in vitro into embryoid bodies (EBs) and in vivo during teratocarcinoma formation. EB formation recapitulates the key developmental processes during peri- and early post-implantation development [41]; these include vascular lineage differentiation and the formation of a network of endothelial cell cords and tubes [22, 42, 43]. The EB system is particularly useful to study loss-of-function mutations when the phenotype is embryonic lethal, as is the case with Vezf1 null embryos.

Our results add new insights into the role of *Vezf1* during vascular development. We observed three major phenotypes in EBs derived from mutant ES cells: delay in growth and attachment, defects in the formation of vascular structures, and extensive and abnormal collagen IV deposition. Importantly, these phenotypes were recapitulated when mutant ES cells were induced to form teratocarcinomas. In contrast to wt EBs that formed a well-organized vascular network surrounded by a defined collagen IV positive ECM, *Vezf1*−/− EBs contained mostly dispersed endothelial cells that failed to form a recognizable network. We also observed reduced angiogenic sprouting and branching in mutant EBs. It is unlikely that these defect are solely a consequence of the slower growth rate of the mutant EBs since overall differentiation was not affected whereas vascular cord formation did not catch up upon extended periods of culture. Rather, it is likely that the defects are the result of differences in endothelial cell polarization, migration and/or alignment. Of interest, intermediate phenotypes were observed in *Vezf1*+/− EBs. Since *Vezf1* mRNA levels are reduced to half in heterozygous EBs, these results provide further support for the notion that *Vezf1* acts in a strictly dosage-dependant fashion.

Loss-of-*Vezf1* gene function resulted in the abnormal distribution and deposition of collagen IV. Loss of collagen IV co-localization with PECAM-1 positive endothelial cells is consistent with the reduced levels of collagen deposition found around capillaries of *Vezf1* null embryos [18]. Collagen IV is a main component of the vascular basement membrane, a specialized ECM on the basal side of endothelial cells, which is important for endothelial differentiation and proliferation and for providing mechanical support [44, 45]. Mice with a targeted inactivation of the Col4α1/2 locus die between E10.5-11.5 due to structural failure of the basement membrane [46]. We propose that loss-of-*Vezf1* causes aberrant accumulation on non-endothelial cells and

incomplete deposition of collagen IV on endothelial cells, resulting in the destabilization of the endothelial basement membrane and the emerging vascular structures, vascular remodeling defects, and the loss of vascular integrity. Importantly, our studies have uncovered retinol/Vitamin A metabolism as a potential molecular pathway linking *Vezf1* function to collagen IV expression and its distribution in the ECM (model in Fig. 2G). Consistent with this model, Vitamin A deficiency in rats has been shown to increase the expression of collagen type IV [47]. We propose that *Vezf1* regulates the retinol/Vitamin A pathway by activating expression of Rbp4 and Ttr. Regulation of Rbp4 and Ttr by *Vezf1* could be achieved either through direct transcriptional transactivation, or indirectly via the transcription factor HNF4α [48].

Previous studies using *Vezf1* antisense RNA resulted in reduced numbers of endothelial cells in G2/M and an increase in apoptosis [14]. In contrast, we did not observe increased apoptosis in *Vezf1*−/− EBs, and therefore apoptosis can be excluded as a cause of the observed angiogenesis defects. Certain metabolic products of collagen IV, including tumstatin [49, 50], and canstatin [51], inhibit angiogenesis by inducing apoptosis. The accumulation of collagen IV in *Vezf1*−/− EBs and teratocarcinomas possibly may be explained by increased local expression and/or low metabolic turnover, which in turn may explain the low number of apoptotic cells.

Unexpectedly, we uncovered striking defects during in vitro differentiation of *Vezf1*-null ES cells along the definitive hematopoietic lineages; in addition, differentiation into primitive erythrocytes was significantly reduced. It should be noted that in *Vezf1* null embryos formation of primitive erythrocytes and megakaryocytes appeared to be normal [18]. However, lethality of homozygous mutant embryos before the onset of definitive hematopoiesis precluded the analysis of potential differentiation defects in vivo.

Histological analyses of teratocarcinomas revealed that loss-of-*Vezf1* does not result in a general block of cell lineage differentiation in these tumors; however, it does affect the tumorigenic ability of ES cells in vivo. Thus, *Vezf1*−/− derived tumors were significantly smaller and displayed an overall less differentiated phenotype, including an increase in neural tubes-like structures, and reduced formation of epithelia with well-defined lumen. It is important to note that significant fewer PECAM-1-positive vascular structures were detected in *Vezf1*−/− teratocarcinomas around and within differentiated tissue structures when compared to wt controls. Lower vascularity may lead to reduced supply of the tumors with nutrients and oxygen, likely resulting in reduced tumor growth. Interestingly, we found that the majority of vascular structures within the tumors were host-derived, whereas ES cell-derived endothelial cells contributed in a mosaic fashion to the vascular cords. Thus, the lower vascular content cannot be attributed solely to reduced differentiation or proliferation of mutant ES cell-derived endothelial structures; rather, differences in angiogenic factors that are present in the tumor microenvironments may play a role as well. It is possible that loss-of-function of *Vezf1* in non-endothelial cells contributes to the observed phenotypes observed in embryoid bodies and teratocarcinomas. However, experimental evidence from the *Vezf1* null mice suggested that endothelial cells are the origin of the primary defects. Results presented here substantiate this notion further: our findings indicate that overall differentiation of ES cells, as judged by cavitation and appearance of cells of the endothelial lineage, is very similar in wt and mutant embryoid bodies.

In conclusion, our studies using the EB and teratocarcinoma model provide new insights into the role of *Vezf1* in the vascular system. Our data further support our hypothesis that *Vezf1* is a transcription factor that controls the formation of a functional three-dimensional vascular network in a strictly dosage-dependant manner. Importantly, they suggest a direct involvement of *Vezf1* in regulating endothelial differentiation, proliferation, and ECM distribution and deposition, with Collagen IV being an important mediator. A complete understanding of how *Vezf1* exerts its role on a molecular level is still lacking. Several potential downstream target

genes have been identified in vitro, these include endothelin-1 [16, 17] and stathmin/OP18 [14]. We have recently performed a microarray screen using RNA from *Vezf1*−/− embryos and identified a small number of potential *Vezf1* target genes; these include members of the retinoic acid metabolism pathway, members of the Apoa/b family of lipid transport proteins, fibrinogens, and members of the serpin family of proteases [28]. In addition, increasing evidence suggests that *Vezf1* function is modulated by protein-protein interactions with components of the Rho GTPase machinery, including RhoB and p68RacGAP [15, 17]. Finally, an intriguing new role for *Vezf1* in epigenetic regulation of gene expression has recently been uncovered [52]. *Vezf1* loss-of-function in ES cells results in down-regulation of the de novo methyltransferase Dnmt3b and affects widespread loss of DNA methylation of genomic DNA. Results from the present study suggest that the embryoid body system will be a powerful in vitro model that will allow studying genetic and epigenetic regulation of vascular system development in a quantitative fashion.

Supplementary Material

Refer to Web version on PubMed Central for supplementary material.

Acknowledgments

We thank Derek Lemons (UCSD) for generating the *Vezf1*$^{lacZ/+}$ targeting vector, W. Blaner (Columbia University) for providing RBP4 antibody and purified RBP4 protein, G. Keller and M. Kennedy (McEwen Centre for Regenerative Medicine) with advice on the hematopoietic progenitor assay, Wendy LeVine for expert technical assistance with histology, and James Mtui for assistance with differentiating ES cells into lymphatic endothelial cells.

Sources of funding. This work was supported by NIH grants R01 HL65738 and R01 HL68648 to H.S., and a post-doctoral fellowship from the Swedish Research Council to P.A.O.

References

1. Carmeliet P. Mechanisms of angiogenesis and arteriogenesis. Nat Med 2000;6:389–395. [PubMed: 10742145]
2. Risau W. Mechanisms of angiogenesis. Nature 1997;386:671–674. [PubMed: 9109485]
3. Carmeliet P, Jain RK. Angiogenesis in cancer and other diseases. Nature 2000;407:249–257. [PubMed: 11001068]
4. Carmeliet P. Angiogenesis in life, disease and medicine. Nature 2005;438:932–936. [PubMed: 16355210]
5. Jain RK. Molecular regulation of vessel maturation. Nat Med 2003;9:685–693. [PubMed: 12778167]
6. Oettgen P. Transcriptional regulation of vascular development. Circ Res 2001;89:380–388. [PubMed: 11532898]
7. Minami T, Aird WC. Endothelial cell gene regulation. Trends Cardiovasc Med 2005;15:174–184. [PubMed: 16165014]
8. Dejana E, Taddei A, Randi AM. Foxs and Ets in the transcriptional regulation of endothelial cell differentiation and angiogenesis. Biochim Biophys Acta 2007;1775:298–312. [PubMed: 17572301]
9. Xiong J-W, Battaglino R, Leahy A, Stuhlmann H. Large-scale screening for developmental genes in ES cells and embryoid bodies using retroviral entrapment vectors. Dev. Dyn 1998;212:181–197. [PubMed: 9626494]
10. Xiong J-W, Leahy A, H-H Lee, Stuhlmann H. *Vezf1*: a Zn finger transcription factor restricted to endothelial cells and their precursors. Dev. Biol 1999;206:123–141. [PubMed: 9986727]
11. Kuhnert F, Stuhlmann H. Identifying early vascular genes through gene trapping in mouse embryonic stem cells. Curr. Top. Dev. Biol 2004;62:261–281. [PubMed: 15522745]
12. Kuhnert, F.; Stuhlmann, H. *Vezf1*: a transcriptional regulator of the endothelium. Cambridge University Press; Cambridge: 2007.

13. Lemons, D.; Sun, X.; Zou, Z.; Campagnolo, L.; Xiong, J-W.; Kuhnert, F.; English, M.; Licht, J.; Stuhlmann, H. VEZF1 is an endothelial transcriptional transactivator that dispays sequence-specific DNA binding to the IL-3, *flk-1* and *flt-1* promoter. 2009. Manuscript under revision
14. Miyashita H, Kanemura M, Yamazaki T, Abe M, Sato Y. Vascular endothelial zinc finger 1 is involved in the regulation of angiogenesis: possible contribution of stathmin/OP18 as a downstream target gene. Arterioscler. Thromb. Vasc. Biol 2004;24:878–884. [PubMed: 15031128]
15. Lebowitz PF, Prendergast GC. Functional interaction between RhoB and the transcription factor DB1. Cell Adhes. Commun 1998;6:277–287. [PubMed: 9865462]
16. Aitsebaomo J, Kingsley-Kallesen ML, Wu Y, Quertermous T, Patterson C. Vezf1/DB1 is an endothelial cell-specific transcription factor that regulates expression of the endothelin-1 promoter. J. Biol. Chem 2001;276:39197–39205. [PubMed: 11504723]
17. Aitsebaomo J, Wennerberg K, Der CJ, Zhang C, Kedar V, Moser M, Kingsley-Kallesen ML, Zeng GQ, Patterson C. p68RacGAP is a novel GTPase-activating protein that interacts with vascular endothelial zinc finger-1 and modulates endothelial cell capillary formation. J. Biol. Chem 2004;279:17963–17972. [PubMed: 14966113]
18. Kuhnert F, Campagnolo L, Xiong JW, Lemons D, Fitch MJ, Zou Z, Kiosses WB, Gardner H, Stuhlmann H. Dosage-dependent requirement for mouse Vezf1 in vascular system development. Dev. Biol 2005;283:140–156. [PubMed: 15882861]
19. Wartenberg M, Gunther J, Hescheler J, Sauer H. The embryoid body as a novel in vitro assay system for antiangiogenic agents. Lab. Invest 1998;78:1301–1314. [PubMed: 9800956]
20. Kearney JB, Bautch VL. In vitro differentiation of mouse ES cells: hematopoietic and vascular development. Methods Enzymol 2003;365:83–98. [PubMed: 14696339]
21. Feraud O, Prandini MH, Vittet D. Vasculogenesis and angiogenesis from in vitro differentiation of mouse embryonic stem cells. Methods Enzymol 2003;365:214–228. [PubMed: 14696348]
22. Vittet D, Prandini MH, Berthier R, Schweitzer A, Martin-Sisteron H, Uzan G, Dejana E. Embryonic stem cells differentiate in vitro to endothelial cells through successive maturation steps. Blood 1996;88:3424–3421. [PubMed: 8896407]
23. Kearney JB, Ambler CA, Monaco KA, Johnson N, Rapoport RG, Bautch VL. Vascular endothelial growth factor receptor Flt-1 negatively regulates developmental blood vessel formation by modulating endothelial cell division. Blood 2002;99:2397–2407. [PubMed: 11895772]
24. Kearney JB, Kappas NC, Ellerstrom C, DiPaola FW, Bautch VL. The VEGF receptor flt-1 (VEGFR-1) is a positive modulator of vascular sprout formation and branching morphogenesis. Blood 2004;103:4527–4535. [PubMed: 14982871]
25. Robertson, EJ. Embryo-derived stem cell lines. In: Robertson, EJ., editor. Teratocarcinomas and embryonic stem cells: a practical approach. IRL Press; Oxford, England: 1987.
26. Liersch R, Nay F, Lu L, Detmar M. Induction of lymphatic endothelial cell differentiation in embryoid bodies. Blood 2006;107:1214–1216. [PubMed: 16195336]
27. Kreuger J, Nilsson I, Kerjaschki D, Petrova T, Alitalo K, Claesson-Welsh L. Early lymph vessel development from embryonic stem cells. Arterioscler Thromb Vasc Biol 2006;26:1073–1078. [PubMed: 16543496]
28. Chitnis, S.; Nichol, D.; Ocaya, PA.; Stuhlmann, H. Gene expression profiling of mouse Vezf1 null embryos. 2010. Submitted
29. Blomhoff R, Blomhoff HK. Overview of retinoid metabolism and function. J Neurobiol 2006;66:606–630. [PubMed: 16688755]
30. von Eynatten M, Humpert PM. Retinol-binding protein-4 in experimental and clinical metabolic disease. Expert Rev Mol Diagn 2008;8:289–299. [PubMed: 18598108]
31. Chang YC, Kao YH, Hu DN, Tsai LY, Wu WC. All-trans retinoic acid remodels extracellular matrix and suppresses laminin-enhanced contractility of cultured human retinal pigment epithelial cells. Exp Eye Res 2009;88:900–909. [PubMed: 19094985]
32. Hellemans K, Grinko I, Rombouts K, Schuppan D, Geerts A. All-trans and 9-cis retinoic acid alter rat hepatic stellate cell phenotype differentially. Gut 1999;45:134–142. [PubMed: 10369717]
33. Qin YH, Lei FY, Hu P, Pei J, Feng ZB, Pang YS. Effect of all-trans retinoic acid on renal expressions of matrix metalloproteinase-2, matrix metalloproteinase-9 and tissue inhibitor of metalloproteinase-1 in rats with glomerulosclerosis. Pediatr Nephrol 2009;24:1477–1486. [PubMed: 19357873]

34. de The H, Vivanco-Ruiz MM, Tiollais P, Stunnenberg H, Dejean A. Identification of a retinoic acid responsive element in the retinoic acid receptor beta gene. Nature 1990;343:177–180. [PubMed: 2153268]
35. Sucov HM, Murakami KK, Evans RM. Characterization of an autoregulated response element in the mouse retinoic acid receptor type beta gene. Proc Natl Acad Sci U S A 1990;87:5392–5396. [PubMed: 2164682]
36. Feraud O, Cao Y, Vittet D. Embryonic stem cell-derived embryoid bodies development in collagen gels recapitulates sprouting angiogenesis. Lab. Invest 2001;81:1669–1681. [PubMed: 11742037]
37. Taylor KL, Henderson AM, Hughes CC. Notch activation during endothelial cell network formation in vitro targets the basic HLH transcription factor HESR-1 and downregulates VEGFR-2/KDR expression. Microvasc. Res 2002;64:372–383. [PubMed: 12453432]
38. Robson P, Stein P, Zhou B, Schultz RM, Baldwin HS. Inner cell mass-specific expression of a cell adhesion molecule (PECAM-1/CD31) in the mouse blastocyst. Dev Biol 2001;234:317–329. [PubMed: 11397002]
39. Keller GM. *In vitro* differentiation of embryonic stem cells. Curr. Opin. Cell Biol 1995;7:862–869. [PubMed: 8608017]
40. Kennedy M, Firpo M, Choi K, Wall C, Robertson S, Kabrun N, Keller G. A common precursor for primitive erythropoiesis and definitive haematopoiesis. Nature 1997;386:488–493. [PubMed: 9087406]
41. Leahy A, Xiong J-W, Kuhnert F, Stuhlmann H. Use of developmental marker genes to define temporal and spatial patterns of differentiation during embryoid body formation. J. Exp. Zool 1999;284
42. Choi K, Chung YS, Zhang WJ. Hematopoietic and endothelial development of mouse embryonic stem cells in culture. Methods Mol. Med 2005;105:359–368. [PubMed: 15492407]
43. Gao F, Shi HY, Daughty C, Cella N, Zhang M. Maspin plays an essential role in early embryonic development. Development 2004;131:1479–1489. [PubMed: 14985257]
44. Madri JA. Extracellular matrix modulation of vascular cell behaviour. Transpl Immunol 1997;5:179–183. [PubMed: 9402683]
45. Paulsson M. Basement membrane proteins: structure, assembly, and cellular interactions. Crit Rev Biochem Mol Biol 1992;27:93–127. [PubMed: 1309319]
46. Poschl E, Schlotzer-Schrehardt U, Brachvogel B, Saito K, Ninomiya Y, Mayer U. Collagen IV is essential for basement membrane stability but dispensable for initiation of its assembly during early development. Development 2004;131:1619–1628. [PubMed: 14998921]
47. Marin MP, Esteban-Pretel G, Alonso R, Sado Y, Barber T, Renau-Piqueras J, Timoneda J. Vitamin A deficiency alters the structure and collagen IV composition of rat renal basement membranes. J Nutr 2005;135:695–701. [PubMed: 15795420]
48. Duncan SA, Nagy A, Chan W. Murine gastrulation requires HNF-4 regulated gene expression in the visceral endoderm: tetraploid rescue of Hnf-4(−/−) embryos. Development 1997;124:279–287. [PubMed: 9053305]
49. Maeshima Y, Colorado PC, Torre A, Holthaus KA, Grunkemeyer JA, Ericksen MB, Hopfer H, Xiao Y, Stillman IE, Kalluri R. Distinct antitumor properties of a type IV collagen domain derived from basement membrane. J Biol Chem 2000;275:21340–21348. [PubMed: 10766752]
50. Sudhakar A, Sugimoto H, Yang C, Lively J, Zeisberg M, Kalluri R. Human tumstatin and human endostatin exhibit distinct antiangiogenic activities mediated by alpha v beta 3 and alpha 5 beta 1 integrins. Proc Natl Acad Sci U S A 2003;100:4766–4771. [PubMed: 12682293]
51. He GA, Luo JX, Zhang TY, Hu ZS, Wang FY. The C-terminal domain of canstatin suppresses in vivo tumor growth associated with proliferation of endothelial cells. Biochem Biophys Res Commun 2004;318:354–360. [PubMed: 15120609]
52. Gowher H, Stuhlmann H, Felsenfeld G. Vezf1 regulates genomic DNA methylation through its effects on expression of DNA methyltransferase Dnmt3b. Genes Dev 2008;22:2075–2084. [PubMed: 18676812]

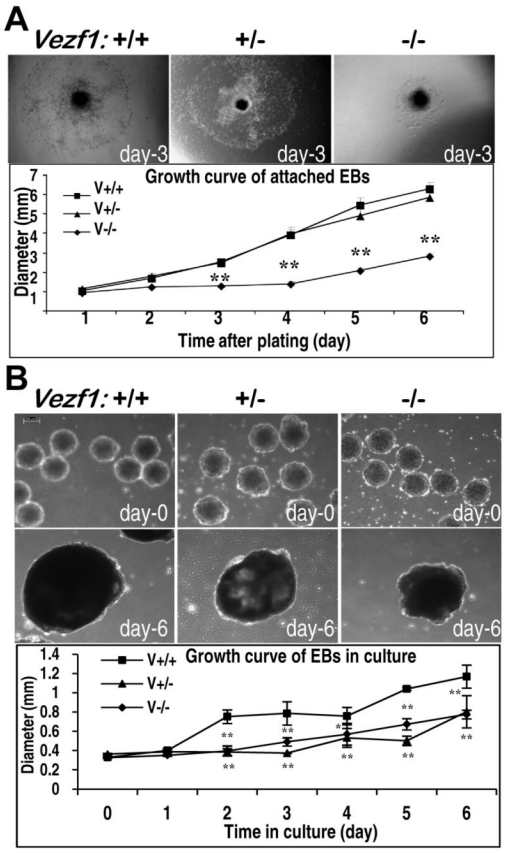

Figure 1. Growth characteristics of wild-type and *Vezf1* mutant embryoid bodies

(A) Growth in 2D attachment culture. EBs were grown for 3 days in suspension culture and switched to 2D attachment culture. EBs attached over night to gelatin-coated plates, and differentiating cells grew out from the center to the periphery. Upper panels: Morphology of representative EBs derived from wt (*Vezf1*+/+), *Vezf1*+/−, and *Vezf1*−/− ES cells, respectively, at day-3 after attachment. Images were taken under an inverted Olympus IX70 microscope. The graph shows growth of EB between day-1 and day-6 of 2D attachment culture. Diameters of EBs (n=14 for each genotype) were measured in 24-hour intervals using Image-Pro Plus software. The experiment was repeated three times, and the graph depicts the results from one representative experiment. **, $P<0.01$ comparison between wt vs. *Vezf1*+/− and wt vs. *Vezf1* +/+ EBs were performed by the student's *t*-test. **(B)** Growth in suspension culture. Upper panels: Representative images of wt, *Vezf1*+/−, and *Vezf1*−/− EBs, respectively, at day-0 and day-6 in suspension culture. Images were taken under a Leica DMIL inverted microscope. Bottom panel: Diameters of EBs in suspension culture were measured from day-0 to day-6 using Leica Application Suite (n=5 for each genotype). Comparison between groups were performed by Two-way ANOVA with Bonferroni post tests. *$P<0.01$, **$P<0.001$ vs. *Vezf1*+/− and *Vezf1*−/− EBs. Data shown as mean ±SEM.

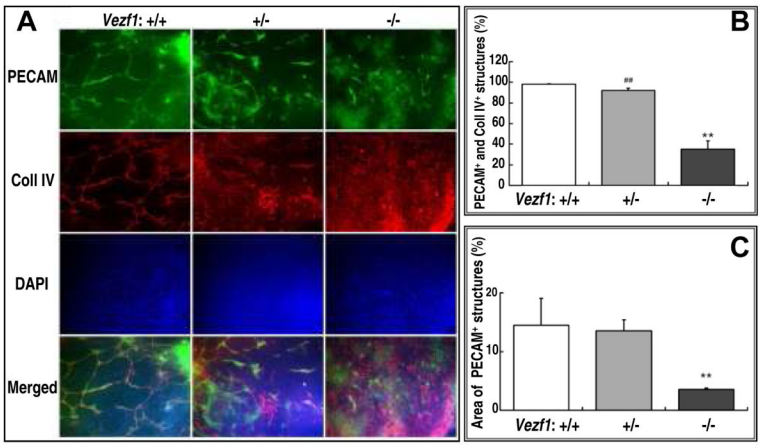

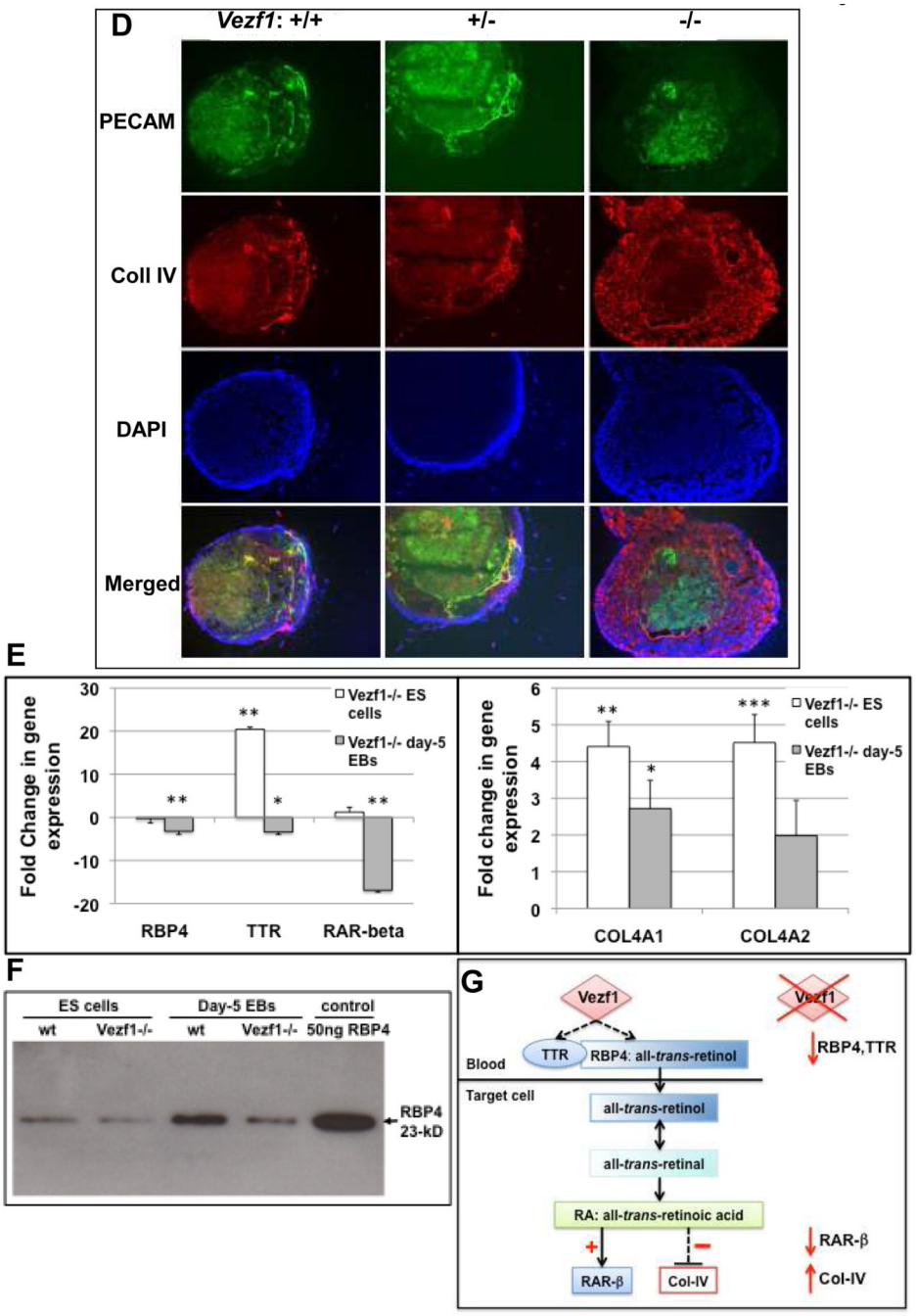

Figure 2. Aberrant vascular structure formation and collagen IV deposition in mutant EBs

(A) EBs in 2D culture Shown are representative images of day-9 EBs derived from wt (*Vezf1* +/+), *Vezf1*+/− and *Vezf1*−/− ES after fixation and immunostaining for PECAM-1 and type IV collagen. Cell nuclei were counter-stained with DAPI. Bottom row depicts merged images from PECAM-1, collagen IV and DAPI staining. Note the extensive vascular network in wt EBs. In contrast, vascular structures did not form properly in *Vezf1*−/− EBs. *Vezf1*+/− EBs displayed an intermediate phenotype. Images were taken under a Zeiss Axioplan 2 IE MOT using a 20x objective.

(B) Quantitative analysis of vascular coverage. The vasculature as shown by PECAM-1^{+} staining was analyzed for area density and expressed as percentage of the PECAM-1^{+} area. At

least three independent measurements were performed in each group. Comparison of *Vezf1*−/− vs. *Vezf1*+/− and *Vezf1*+/+ groups were performed by student's *t*-test; **, $P<0.01$. **(C)** Quantitative analysis of co-expression of PECAM-1 and collagen IV. Shown is the percentage of collagen IV^+ areas that was adjacent to or overlapped with PECAM-1^+ areas. Comparisons between two groups were done using student's *t*-test. **, $P<0.01$ *Vezf1*−/− vs. *Vezf1*+/+; $^{\#\#}$, $P<0.01$ *Vezf1*−/− vs. *Vezf1*+/−.

(D) Suspension culture EBs. Sections of EBs grown for 9 days in suspension culture were immunostained for PECAM-1 and collagen IV. Cell nuclei were counter-stained with DAPI. Bottom row depicts merged images from PECAM-1, collagen IV and DAPI staining. Well-developed PECAM-1 and collagen IV positive vascular structures were visible in wt and, to a lesser degree, in *Vezf1*+/− EBs. In *Vezf1*−/− EBs, PECAM-1 positive sheets of cells were visible in the center, but these failed to form cell cords and they did not co-stain with collagen IV.

(E) Expression of retinol pathway genes Rbp4, Ttr, and RAR-β, and collagen 4a1 and 4a2 in ES cells and embryoid bodies. Gene expression levels were determined by quantitative RT-PCR and normalized to β-actin. Shown are changes in expression in *Vezf1*−/− vs. wt ES cells and day-5 EBs. Comparisons between wt and Vezf1−/− ES cells and EBs were performed by student's *t*-test (n=3 for each genotype).

(F) Detection of secreted RBP4 protein by western blot analysis. Representative western blot using conditioned media (50μg protein) from wt and *Vezf1*−/− ES cells and day-5 EBs. 50 ng of purified 23-kD RBP4 protein was loaded as a control. RBP4 levels are reduced in *Vezf1*−/− EBs and, to a lesser extent, in *Vezf1*−/− ES cells.

(G) Model proposing how *Vezf1* regulates the retinol/Vitamin A pathway. Left: *Vezf1* activates expression of the all-trans retinol carrier Rbp4 and transthyretin, directly or indirectly. TTR binds to RBP4:all-trans retinol, preventing its renal clearance and resulting in increased cellular uptake. Retinol is converted to retinal and retinoic acid, which directly transactivates expression of its receptor RAR-β and indirectly represses that of Collagen IV. Right: Loss of *Vezf1* function in EBs results in deregulation of the retinol/Vitamin A pathways with reduced expression of Rbp4, Ttr and RAR-β, and accumulation of collagen IV.

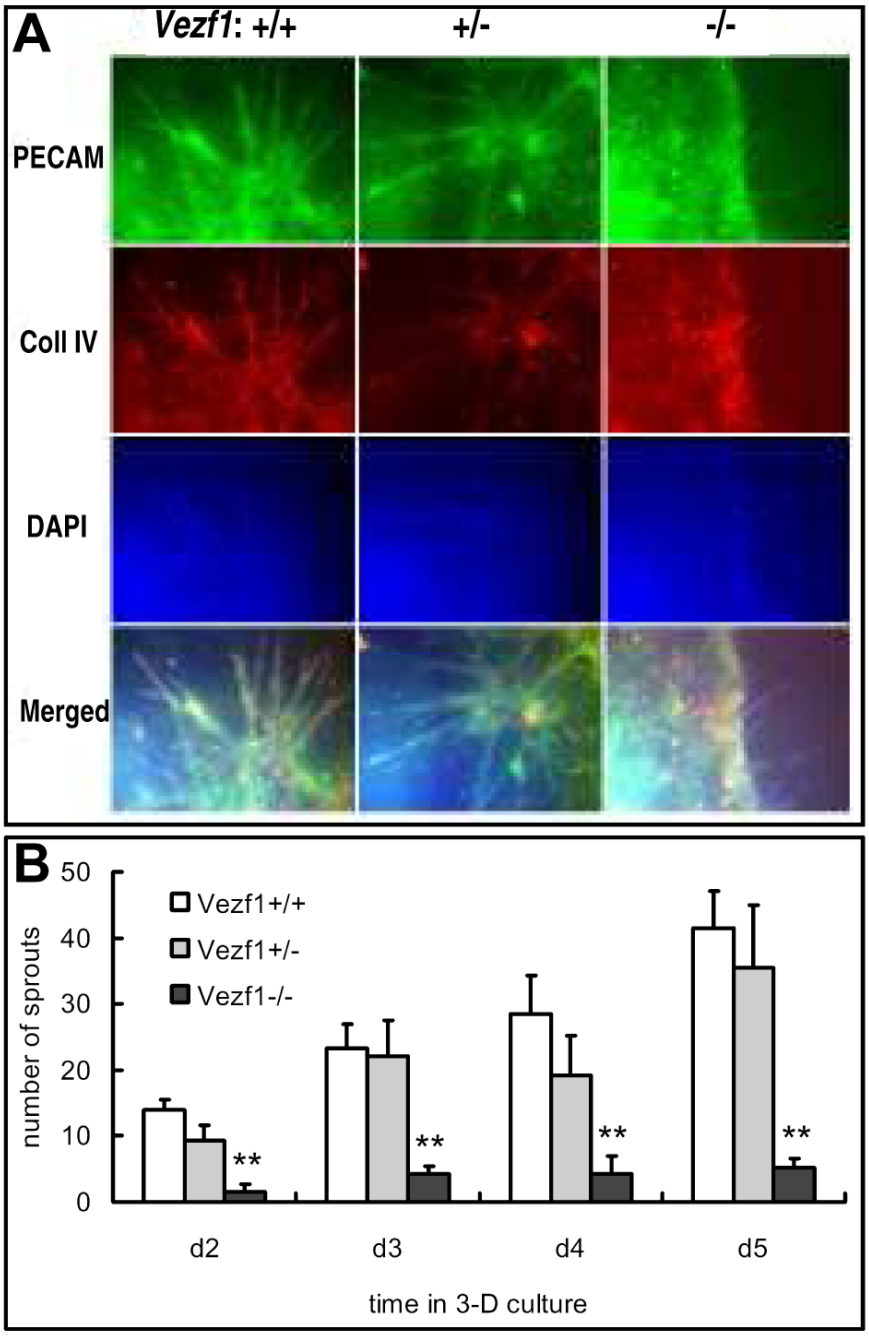

Figure 3. Vascular sprout formation in EBs cultured in collagen matrix

(A) EBs were cultured for 12 days in suspension culture, followed by 5-day culture in collagen type I gel drops. Endothelial cell sprouts were visualized by whole-mount staining of embedded EBs for PECAM-1 and type IV collagen. Cell nuclei were counter-stained with DAPI. Bottom row depicts merged images from PECAM-1, collagen IV and DAPI staining. Sprout formation was significantly impaired in *Vezf1*−/− EBs when compared to wt and *Vezf1*+/− EBs. **(B)** Quantitative analysis of vascular sprout formation. Individual vascular sprouts from EBs, as indicated by PECAM-1^+ staining in corresponding images, were counted at day 2, 3, 4 and 5 in collagen drops (n=10 from each genotype). Comparison of *Vezf1*−/− vs. *Vezf1*+/− and *Vezf1* +/+ groups were performed by student's *t*-test; **, $P<0.01$.

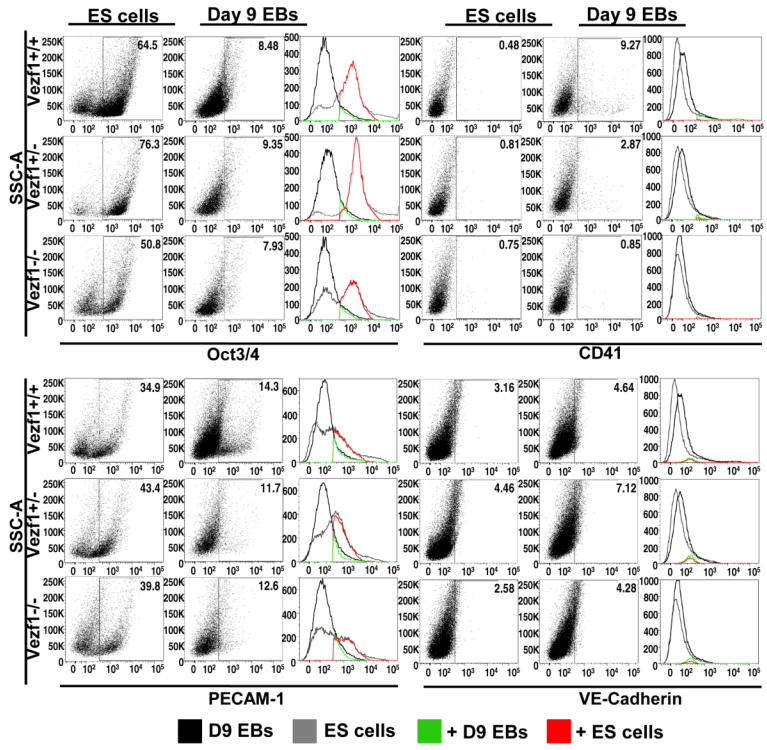

Figure 4. Analysis of Oct3/4, CD41, PECAM-1, and VE-Cadherin gene expression in undifferentiated ES cells and differentiated cells from day-9 EBs

Wild-type, *Vezf1*+/−, and *Vezf1*−/− ES cells (10^6 cells each) and dissociated cells from day-9 suspension culture EBs (550, 880, and 3,300 EBs from wt, *Vezf1*+/−, and *Vezf1*−/− EBs, respectively) were analyzed by flow cytometry for the expression of Oct3/4, CD41, PECAM-1 and VE-Cadherin. The gates correspond to Oct3/4+, CD41+, PECAM-1+ or VE-Cadherin+ populations. The histograms depict the number of day-9 EB-derived cell population (black), ES cell population (grey), positive cells from day 9 EB cell population (green), and positive cells from the ES cell population (red).

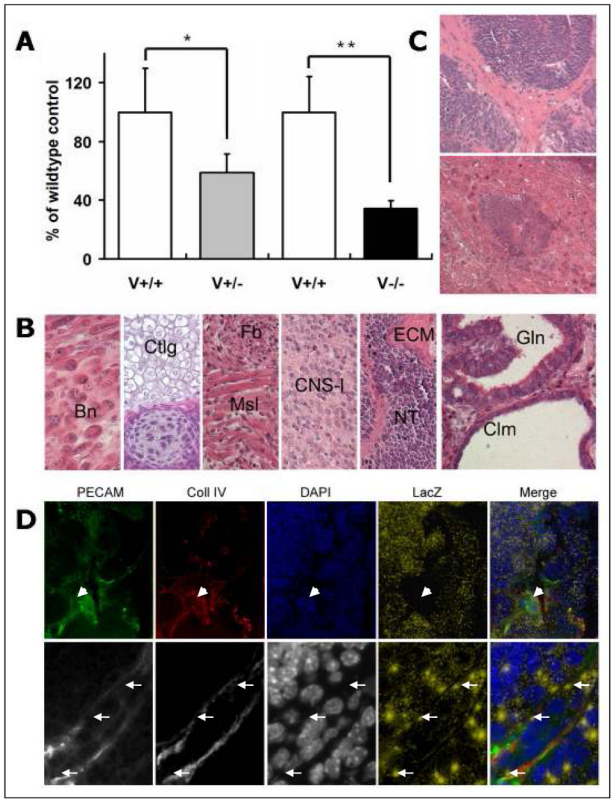

Figure 5. Teratocarcinoma formation in nude mice

(A) Comparison of weight of teratocarcinomas derived from *Vezf1*+/− and *Vezf1*−/− ES cells with their wt controls 2 weeks after subcutaneous injection. The weight of each individual teratocarcinoma was expressed as a percentage of the control (100%) co-injected into the same animal. Six mice each were used for *Vezf1*+/− and *Vezf1*−/− ES cells. *Vezf1*+/− and *Vezf1*−/− teratocarcinomas were significantly smaller than the wt controls. Values are shown as mean ±SE. Comparisons between two groups were performed using student's *t*-test. * $P<0.05$; wt vs. *Vezf1*+/−, ** $P<0.01$ wt vs. *Vezf1*−/−. **(B)** Histology of representative H&E stained sections of *Vezf1*−/− teratocarcinomas. From left to right: Bn, bone; Ctlg, cartilage; Fb, fibroblasts; Msl, muscle; CNS-l, central nervous system-like tissue; ECM, extracellular matrix; NT, neural tube; Gln, gland; Clm, cilium. **(C)** *Vezf1*−/− teratocarcinomas contained an abundance of areas with less differentiated tissues: multi-cell layered neural tube-like structures with more increased cellularity and decreased lumen formation (top), and extensive deposition of extracellular matrix surrounding neural tube structures (top), or within bone-like structures (bottom). **(D)** Cryosections of $Vezf1^{lacZ/+}$ ES cell-derived teratocarcinomas were stained for PECAM-1 and collagen IV, and β-galactosidase. Cell nuclei were counterstained with DAPI. To visualize lacZ in the merged pictures, β-galactosidase staining was shown in a pseudocolor (yellow dots). Most of the PECAM-1, collagen IV positive vessels were negative for lacZ (arrow head). A small fraction of blood vessels contained cells that showed β-galactosidase expression (arrow). Top: 20x objective; bottom: 63x objective.

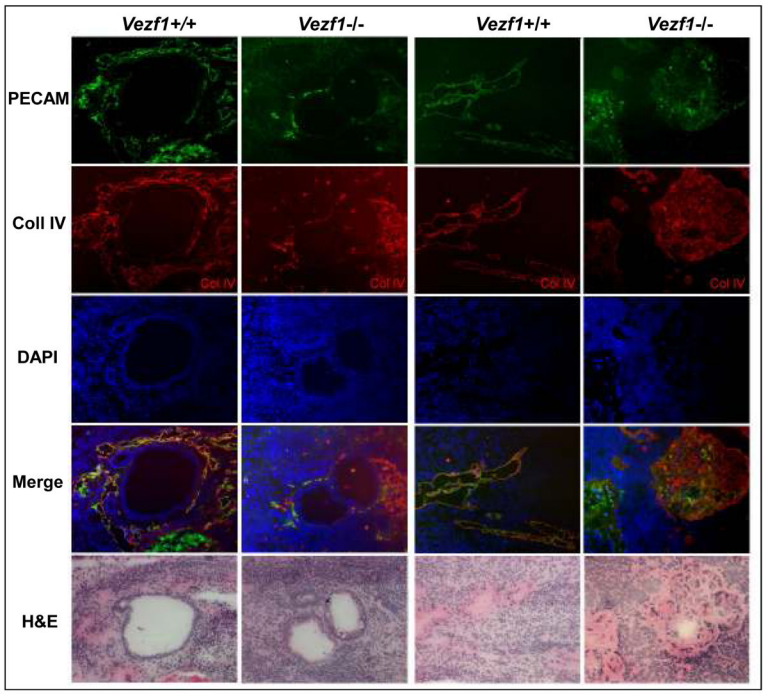

Figure 6. Vascular structure defects in *Vezf1*−/− teratocarcinomas

Representative sections from 2 wt and 2 contra-lateral Vezf1−/− teratocarcinomas are shown. Sections were immunostained for PECAM-1 and collagen IV, and cell nuclei were counterstained with DAPI. Merged images are from single PECAM-1, collagen IV and DAPI images. Bottom row: close-by H&E stained section. Note the absence of well-formed vascular structures around glandular epithelial structures in *Vezf1*−/−, but not wt teratocarcinomas (left 2 columns). Mesenchyme-rich areas in wt teratocarcinomas contained PECAM-1, collagen IV positive vessels. In contrast, Vezf1−/− teratocarcinomas contained large mesenchymal foci with high collagen IV deposition and much lower PECAM-1 expression. These areas did not contain recognizable vascular structures (right 2 columns).